Glycobiology and Extracellular Matrices:

Leishmania UDP-sugar Pyrophosphorylase: THE MISSING LINK IN GALACTOSE SALVAGE?

Sebastian Damerow, Anne-Christin Lamerz, Thomas Haselhorst, Jana Führing, Patricia Zarnovican, Mark von Itzstein and Françoise H. Routier

J. Biol. Chem. 2010, 285:878-887.
doi: 10.1074/jbc.M109.067223 originally published online November 11, 2009

THE JOURNAL OF BIOLOGICAL CHEMISTRY VOL. 285, NO. 2, pp. 878–887, January 8, 2010

Leishmania UDP-sugar Pyrophosphorylase

THE MISSING LINK IN GALACTOSE SALVAGE?[S]

Received for publication, September 17, 2009, and in revised form, November 9, 2009 Published, JBC Papers in Press, November 11, 2009, DOI 10.1074/jbc.M109.067223

Sebastian Damerow[‡], Anne-Christin Lamerz[‡1], Thomas Haselhorst[§], Jana Führing[‡], Patricia Zarnovican[‡], Mark von Itzstein[§2], and Françoise H. Routier[‡3]

From the [‡]Department of Cellular Chemistry, Hannover Medical School, Carl-Neuberg-Strasse 1, 30625 Hannover, Germany and the [§]Institute for Glycomics, Griffith University (Gold Coast Campus), Parklands Drive, Southport, Queensland 4222, Australia

The *Leishmania* parasite glycocalyx is rich in galactose-containing glycoconjugates that are synthesized by specific glycosyltransferases that use UDP-galactose as a glycosyl donor. UDP-galactose biosynthesis is thought to be predominantly a *de novo* process involving epimerization of the abundant nucleotide sugar UDP-glucose by the UDP-glucose 4-epimerase, although galactose salvage from the environment has been demonstrated for *Leishmania major*. Here, we present the characterization of an *L. major* UDP-sugar pyrophosphorylase able to reversibly activate galactose 1-phosphate into UDP-galactose thus proving the existence of the Isselbacher salvage pathway in this parasite. The ordered bisubstrate mechanism and high affinity of the enzyme for UTP seem to favor the synthesis of nucleotide sugar rather than their pyrophosphorolysis. Although *L. major* UDP-sugar pyrophosphorylase preferentially activates galactose 1-phosphate and glucose 1-phosphate, the enzyme is able to act on a variety of hexose 1-phosphates as well as pentose 1-phosphates but not hexosamine 1-phosphates and hence presents a broad *in vitro* specificity. The newly identified enzyme exhibits a low but significant homology with UDP-glucose pyrophosphorylases and conserved in particular is the pyrophosphorylase consensus sequence and residues involved in nucleotide and phosphate binding. Saturation transfer difference NMR spectroscopy experiments confirm the importance of these moieties for substrate binding. The described leishmanial enzyme is closely related to plant UDP-sugar pyrophosphorylases and presents a similar substrate specificity suggesting their common origin.

Trypanosomatid parasites of the genus *Leishmania*, the causal agent of the human disease leishmaniasis, are characterized by a digenetic life cycle with a promastigote stage in the sandfly vector and an amastigote stage in mammalian macrophages. According to World Health Organization reports, more than 20 million people are infected worldwide and present manifestations ranging from self-healing cutaneous lesions to fatal visceral forms.

Leishmania parasites are coated by a dense glycocalyx composed of glycosylphosphatidylinositol-like structures, which is essential for parasite survival in the sandfly vector and, at least for some species, for promastigote infectivity in the mammalian host (1). This glycocalyx is particularly rich in galactose occurring either in the pyranosic form (Gal) or the more unusual furanosic form (Gal*f*).[4] Its biosynthesis thus depends on the availability of the nucleotide-activated sugar UDP-galactopyranose (UDP-Gal), which can be interconverted into UDP-galactofuranose (UDP-Gal*f*) by the specific enzyme UDP-galactopyranose mutase (2, 3). Consequently, mutants deficient in the formation of UDP-Gal*f* or in the transport of UDP-Gal into the secretory pathway organelles present an altered glycocalyx associated with parasite attenuation (4–7). A route to UDP-Gal formation is via epimerization of the abundant nucleotide sugar UDP-glucose (UDP-Glc) by the UDP-Glc 4-epimerase (8). The biosynthesis of UDP-Gal is thus intimately linked to glucose metabolism (Fig. 1). Because the trypanosomatid parasites *Trypanosoma brucei* and *Trypanosoma cruzi* are unable to take up galactose from the environment (9, 10), the UDP-Glc 4-epimerase is indispensable for biosynthesis of UDP-Gal and derived glycoconjugates in these organisms and is essential for their survival (11–14). In contrast, a salvage pathway for UDP-Gal synthesis is known to occur in *Leishmania* because radiolabeled Gal is taken up by promastigotes and incorporated into surface molecules (15). Gal most likely enters cells by a family of hexose transporters (16) before being converted into galactose 1-phosphate (Gal-1-P) by the putative galactokinase present in the genome (*LmjF*35.2740). Deletion of three of these hexose transporters in *Leishmania mexicana* revealed their importance in the growth, infectivity, and survival of the parasite underlining the importance of monosaccharide salvage in both promastigotes and amastigotes (16, 17).

Gal-1-P is usually activated into UDP-Gal by a UDP-glucose: α-D-galactose-1-phosphate uridylyltransferase enzyme (EC 2.7.7.12 encoded by the gene GALT) via the Leloir pathway. A clear homologue of this activating enzyme is, however, not found in the *Leishmania major* genome. Alternatively, incorporation of Gal-1-P into uridine nucleotide by a pyrophospho-

[S] The on-line version of this article (available at http://www.jbc.org) contains supplemental Figs. S1–S5.

The nucleotide sequence(s) reported in this paper has been submitted to the GenBank™/EBI Data Bank with accession number(s) EU249268.

[1] Present address: Roche Diagnostics GmbH, Sandhofer Strasse 116, 68305 Mannheim, Germany.

[2] Recipient of support from the Australian Research Council and the National Health and Medical Research Council.

[3] To whom correspondence should be addressed. Tel.: 49-511-532-9807; Fax: 49-511-532-3947; E-mail: Routier.Francoise@mh-hannover.de.

[4] The abbreviations used are: Gal*f*, galactofuranose; GalA, galacturonuic acid; GALT, UDP-glucose:α-D-galactose-1-phosphate uridylyltransferase; STD, saturation transfer difference; UGP, UDP-glucose pyrophosphorylase; USP, UDP-sugar pyrophosphorylase.

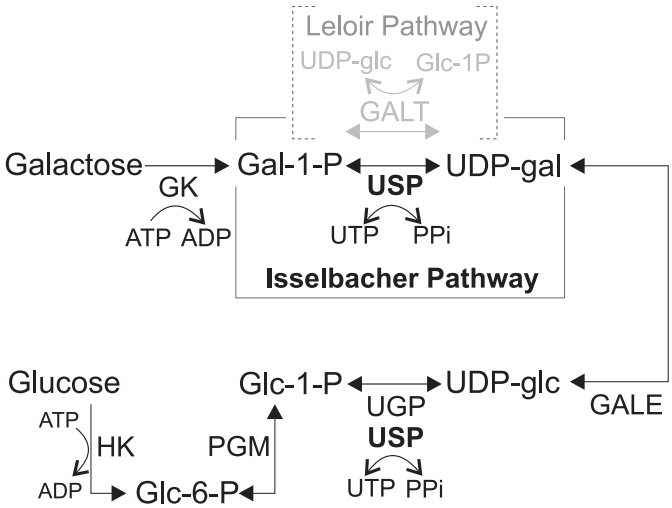

FIGURE 1. **UDP-galactose synthesis in *L. major*.** The abbreviations used are as follows: *GK*, galactokinase (EC 2.7.1.6); *USP*, UDP-sugar pyrophosphorylase (EC 2.7.7.64); *GALT*, UDP-glucose:α-D-galactose-1-phosphate uridylyltransferase; *GALE*, UDP-galactose 4-epimerase (EC 5.1.3.2); *UGP*, UDP-glucose pyrophosphorylase (EC 2.7.7.9); *PGM*, phosphoglucomutase (EC 5.4.2.2); and *HK*, hexokinase (EC 2.7.1.1). The *GALT* gene is absent from *L. major* genome suggesting the absence of the Leloir pathway.

rolytic reaction has been reported in mammals and constitutes the Isselbacher pathway (Fig. 1) (18), although a UTP:α-D-galactose-1-phosphate uridylyltransferase (EC 2.7.7.10) has never been identified. In stark contrast, plants exhibit an enzyme with broad specificity called UDP-sugar pyrophosphorylase (USP; EC 2.7.7.64) that has been recently involved in this alternative pathway for Gal activation (19–21).

Analysis of an L. *major* UDP-glucose pyrophosphorylase (UGP) deletion mutant[5] revealed the presence of Gal-containing molecules underlining the existence of a UDP-Gal biosynthetic pathway independent of UDP-Glc biosynthesis. Here, we report the identification, cloning, and characterization of an *L. major* UDP-sugar pyrophosphorylase (USP) (EC 2.7.7.64) with broad substrate specificity, including Gal-1-P and glucose 1-phosphate (Glc-1-P). The enzyme identified by homology with its plant orthologues (19, 21) suggests the presence of the Isselbacher pathway in *Leishmania*.

EXPERIMENTAL PROCEDURES

Cloning, Expression, and Purification of His_6-tagged L. major USP—The entire open reading frame of *L. major* UDP-sugar pyrophosphorylase (*LmjF*17.1160) was amplified with the primer set ACL115 (CTG ACT CCA TAT GAC GAA CCC GTC CAA CTC C) and ACL116 (CTT AGC GGC CGC ATC AAC TTT GCC GGG TCA GCC G), containing integrated restriction sites for NdeI and NotI, respectively, and inserted into a pET22b expression vector (Novagen), containing a C-terminal His_6 tag. For recombinant expression, the vector was transformed into Ca^{2+}-competent *Escherichia coli* BL21(DE3) via heat shock. Cells were grown in Power Broth (AthenaES) at 37 °C to an absorbance of 1.0 and transferred to 15 °C. The expression was induced at an absorbance of 1.2 by addition of 1 mM isopropyl 1-thio-β-D-galactopyranoside. After 20 h, the cells were harvested by centrifugation (6000 × *g*, 15 min, 4 °C) and washed with phosphate-buffered saline.

A bacterial pellet obtained from 500 ml of Power Broth solution was resuspended in 15 ml of Ni^{2+}-chelating buffer A_{Ni} (50 mM Tris/HCl, pH 7.8, 300 mM NaCl), including protease inhibitors (40 μg/ml bestatin (Sigma), 4 μg/ml pepstatin (Sigma), 0.5 μg/ml leupeptin (Serva), and 1 mM phenylmethylsulfonyl fluoride (Roche Applied Science)). Cells were lysed by sonication with a microtip (Branson Sonifier, 50% duty cycle, output control 5, eight 30-s pulses for 8 min), and cell debris was removed by centrifugation (20,000 × *g*, 15 min, 4 °C). The soluble fraction was loaded onto a 1-ml HisTrap HP Ni^{2+}-chelating column (GE Healthcare). After a 20-ml wash with buffer A_{Ni} (50 mM Tris/HCl, pH 8, 300 mM NaCl), the column was eluted with 20 ml of buffer A_{Ni} containing 40 mM imidazole followed by a final elution step of 5 ml of buffer A_{Ni} containing 300 mM imidazole. The fractions containing *L. major* USP were pooled and passed over a HiPrep 26/10 desalting column (GE Healthcare) to exchange buffer A_{Ni} to buffer A_Q (50 mM Tris/HCl, pH 8.0). The sample was then loaded on a 1-ml Q-Sepharose FF anion-exchange column (GE Healthcare) that was successively washed and eluted with 20 ml of buffer A_Q, 20 ml of buffer A_Q containing 100 mM NaCl, and a final volume of 5 ml of buffer A_Q containing 300 mM NaCl. Again, the fractions containing the recombinant *L. major* USP were pooled and exchanged to standard buffer (Tris/HCl, pH 7.8, 10 mM $MgCl_2$) via HiPrep 26/10 column. Purified samples were snap-frozen in liquid nitrogen and stored in standard buffer at −80 °C.

Complementation of E. coli DEV6 galU Mutant—Complementation of the *E. coli* DEV6 galU mutant strain was performed as described previously by Lamerz *et al.* (22).

Size-exclusion Chromatography—Size-exclusion chromatography on a Superdex 200 10/300 GL column (10 × 300 mm) (GE Healthcare) was used to determine the quaternary organization of the recombinant *L. major* USP. The column was equilibrated with 50 ml of standard buffer (50 mM Tris/HCl, pH 7.8, 10 mM $MgCl_2$ loaded with 100 μl of one of the following standard proteins: bovine carbonic anhydrase (3 mg/ml), bovine serum albumin (10 mg/ml), yeast alcohol dehydrogenase (5 mg/ml), potato β-amylase (4 mg/ml), and thyroglobulin (3 mg/ml) (protein standard kit; Sigma) or with purified recombinant His_6-tagged *L. major* USP (4 mg/ml) and eluted at a flow rate of 1 ml/min. The apparent molecular weight was determined by standard curve.

In Vitro Enzyme Assays—The formation of pyrophosphate in the forward reaction was detected with the EnzChek® pyrophosphate assay kit (Molecular Probes). The assay medium contained 50 mM Tris/HCl, pH 7.8, 10 mM $MgCl_2$, 1 mM dithiothreitol, 0.2 mM 2-amino-6-mercapto-7-methylpurine ribonucleoside, 0.03 units of inorganic pyrophosphatase, 2.0 units of purine nucleoside phosphorylase, and varying amounts of sugar 1-phosphate and UTP ranging from 0.5 to 3 mM. Enzyme reactions were performed at 25 °C in a total volume of 100 μl and started by the addition of USP. A control without USP was used for normalization.

UTP produced in the reverse reaction was converted into 1 eq of inorganic phosphate by *E. coli* CTP-synthase in presence

[5] A.-C. Lamerz, S. Damerow, B. Kleczka, M. Wiese, G. van Zanbergen, A. Wenzel, J. Lamerz, F. F. Hsu, J. Turk, S. M. Beverley, and F. H. Routier, unpublished work.

of ATP, L-Gln, and the cofactor GTP. Inorganic phosphate was then quantified using the EnzChek® pyrophosphate assay kit (Molecular Probes) but omitting the first coupling enzyme. For these experiments, the CTP-synthase gene was recombinantly cloned from *E. coli* XL1-blue in a pET22b expression vector with a primer set, including NdeI and NotI restriction sites (SD13, CTT ACA TAT GCA TCA TCA TCA TCA TCA CGC TAG CGG ATC CAT GAC AAC GAA CTA TAT TTT TGT GAC C; SD14, CTT AGC GGC CGC TTA CTT CGC CTG ACG TTT CTG G). The N-terminal His-tagged CTP-synthase was expressed and purified as described above for the USP but without anion-exchange chromatography. The assay mixture for the reverse reaction contained 50 mM Tris/HCl, pH 7.8, 10 mM $MgCl_2$, 1 mM dithiothreitol, 0.2 mM 2-amino-6-mercapto-7-methylpurine ribonucleoside, 1 mM ATP, 1 mM L-Gln, 0.25 mM GTP, 3 μg of CTP-synthase, 2.0 units of PNP, and 2 mM UDP-sugar and pyrophosphate in a final volume of 100 μl. The reaction was initiated by addition of USP and normalized to buffer control.

Measurements were performed in 96-well half-area flat-bottom microplates (Greiner Bio-One) with the Power-Wave™ 340 KC4 system (Bio-Tek). To exclude cross-reactions, all substrates and cofactors of coupling enzymes were tested against USP inhibition or competition and vice versa (data not shown). The determinations of K_m and V_{max} values were performed using varying substrate concentrations up to 12 triplicates, whereas the second substrate was set to a constant saturating concentration. The initial linear rates (y) were plotted against the substrate concentrations (x), and the Michaelis-Menten kinetics was analyzed in PRISM using nonlinear regression ($y = V_{max} \cdot x/(K_m + x)$).

SDS-PAGE Analysis and Immunoblotting—SDS-PAGE was performed according to Laemmli. Protein samples were separated on SDS-polyacrylamide gels composed of a 5% stacking gel and a 10% separating gel. Protein bands were visualized by Coomassie Brilliant Blue staining. For Western blot analysis, proteins were transferred to nitrocellulose membranes (Schleicher & Schüll). His_6-tagged proteins were detected using the penta-His antibody (Qiagen) at a concentration of 1 μg/ml and a goat anti-mouse Ig alkaline phosphatase conjugate (Jackson ImmunoResearch).

STD NMR—All STD NMR experiments were performed on a Bruker Avance DRX 600 MHz spectrometer equipped with a triple axis cryoprobe at 298 K in 50 mM deuterated Tris buffer, pH 7.8, and 10 mM $MgCl_2$. The protein was saturated with a cascade of 40 selective Gaussian-shaped pulses of 50 ms duration with a 100-μs delay between each pulse resulting in a total saturation time of ~2 s. The on- and off-resonance frequency was set to 0.7 and 40 ppm, respectively. In a typical STD NMR experiment, 0.5 μM recombinant USP was used, and all investigated ligands were added at a molecular ratio (protein/ligand) of 1:100. A total of 1024 scans per STD NMR experiment were acquired, and a WATERGATE sequence was used to suppress the residual HDO signal. A spin lock filter with strength of 5 kHz and duration of 10 ms was applied to suppress protein background. Relative STD effects were calculated according to the equation $A_{STD} = (I_0 - I_{sat})/I_0 = I_{STD}/I_0$ by comparing the intensity of the signals in the STD-NMR spectrum (I_{STD}) with signal intensities of a reference spectrum (I_0). The STD signal with the highest intensity was set to 100%, and other STD signals were calculated accordingly (23).

RESULTS

Identification of a Putative UDP-sugar Pyrophosphorylase in Leishmania Genome—Although enzymatic epimerization of UDP-glucose is clearly not the sole source of UDP-galactose in *Leishmania major* (15),[5] the genome of this parasite lacks an obvious UDP-glucose:α-D-galactose-1-phosphate uridylyltransferase enzyme (EC 2.7.7.12). BLAST searches of the *L. major* genome revealed, however, the existence of a gene (*LmjF*17.1160) displaying ~32% identity with pea sprout USP (19) and 15% identity with *L. major* UGP (22, 24). This gene is extremely conserved among *Leishmania* species and is also found in *T. cruzi* but not in *T. brucei*. In *L. major*, the encoded protein referred to here as *L. major* USP or *Lmj*USP contains 630 amino acids and has a theoretical molecular mass of 69 kDa. An alignment of *L. major* USP and UGP is presented in Fig. 2*A* and highlights the conservation of residues essential for catalytic activity of pyrophosphorylase and for nucleotide sugar binding (25, 26). The *Lmj*USP basic residues Lys-134, His-224, and Lys-434 (corresponding to *Lmj*UGP Lys-95, His-191, and Lys-380) are strictly conserved and predicted to be involved in phosphate binding (26). Similarly, with the exception of Val-120, which is a lysine residue in UGPs, the amino acids involved in uridine binding are preserved. In contrast, only two of the residues of UGPs interacting with the glucose moiety (Gly-256 and Asn-308) are conserved in USPs (Fig. 2*A* and supplemental Fig. S1).

The phylogenetic tree presented in Fig. 2*B* demonstrates that *Lmj*USP is clearly distinct from the UDP-Glc-synthesizing enzyme UGP as well as the UDP-*N*-acetylglucosamine pyrophosphorylase and UDP-glucose:α-D-galactose-1-phosphate uridylyltransferase (GALT). Trypanosomatid USPs clusters with the plant and algal USPs but constitute a separate branch.

L. major USP Is Involved in Biosynthesis of UDP-glucose and/or UDP-galactose—To demonstrate the role of *L. major* putative USP in the metabolism of galactose, we first investigated its ability to complement the growth defect of *E. coli* galU mutant strain DEV6. This specific bacterial strain is unable to grow on agar-containing galactose as the only carbohydrate source due to a mutation in UGP, which prevents synthesis of UDP-Glc and subsequent depletion of the cytotoxic Gal-1-P by the UDP-glucose:α-D-galactose-1-phosphate uridylyltransferase enzyme. Upon transformation with *Lmj*USP cDNA, the ability of these bacteria to grow on galactose-containing media was restored (supplemental Fig. S2) indicating the involvement of *L. major* USP in the activation of Gal-1-P either dependently (via the Leloir pathway) and/or independently of UDP-Glc biosynthesis (via the Isselbacher pathway) (Fig. 1).

L. major USP Is a Monomer Exhibiting Broad Substrate Specificity—Oligomerization has been shown to regulate the activity of barley UGP (27) but not that of *L. major* UGP (22). We have thus investigated the oligomerization state of *L. major* C-terminally His-tagged USP (*Lmj*USP-His_6) expressed in *E. coli* BL21 (DE3) cells and purified to homogeneity via nickel affinity, anion-exchange, and size-exclusion chromatographies

A

```
USP   1   MTNPSNSNLQALREELCTPGLDQGHLFEGWPETVDECNERQIALLTDLYMFSNMYPGGVAQYIRNGHELLARESEEVDFA  80
UGP   1   MENDMKS--LSAAAQACVKKMRDAKVNE----------ACIRTFIAQHVMVSKGETG----------------------  45

USP  81   ALEMPPLLIFEAPSLHRRTAERTALENAGTAM--LCKTVFVLVAGGLGERLGYSSIKVSLPV-ETATNTTYLAYYLRWAQR  157
UGP  45   ------SLPDSAIMPVDSLDALDSLTIECDNAVLQSTVVLKLNGGLGTGMGLCDAKTLLEVKDGKTFLDFTALQVQYLRQ  119

USP 158   VGGKEVPFVIMTSDDTHDRTLQLLRE-----LQLEVPNLHVLKQGQVFCFADSAAHLALDETGK-LLRKPHGHGDVHSLI  231
UGP 120   HCSEHLRFMLMDSFNTSASTKSFLKARYPWLYQVFDSEVELM-QNQVPKILQDTLEPAAWAENPAYEWAPPGHGDIYTAL  198

USP 232   YNATVKRDVVPDSGDGTATAQPLVNDWLAAGYESIVFIQDTNAGATITIPISLALSAEHSLDMNFTCIPRVPKEPIGLLC  311
UGP 199   YGSGK----------------LQELVEQGYRYMFVSNGDNLGATIDKRVLA-YMEKEKIDFLMEVCRRTESDKKGGHL  259

USP 311   --RTKKNSGDPWLVANVEYNVFAEVSRALNKDGGDEVSDPTGFSPFPGSVNTLVFKLSSYVDRLRESHGI--VPEFINPK  387
UGP 260   ARQTVYVKGKDGQPDAEKRVLLLRESAQCPKADMESFQDINKYSF--FNTNNLWIRLPVLLETMQEHGGTLPLPVIRNEK  337

USP 388   YSDETRRSFKKPARIESLMQDIALLFSEDDYRVGGTVFERFSYQPVKNSLEEAAGLVAQGNGAYCAATGEAAFYELQRRR  467
UGP 338   TVDSSNSASPKVYQLETAMGAAIAMF-ESASAIVVPRSR---FAPVKTCADLLALRSDAY------                393

USP 468   LKAIGLPLFYSSQPEVTVAKDAFGVRLFPIIVLDTMCASSGSLDDLARVFPTPEKVHIDQHSTLIVEGRV-IIESLELYG  546
UGP 393   ------VVTDDFRLVLDDRCHGHP----PVVDLDSAHYKMMNGFEKLVQHGVPSLVE---CKRVTVKGLVQFGAGNVLTG  460

USP 547   ALTIRGPTDSMALPHVVRNAVVRNAGWSVHAILSLCAGRDSRLSEVDRIRGFVLKKTAMAVMDCNTKGESEAGAPSGAAD  626
UGP 461   TVTIE-NTDSASAFVIPDGAKLN----------------------------------------DTTASPQQSTNK-----  494

USP 627   PAKL  630
UGP 494   ----  494
```

B

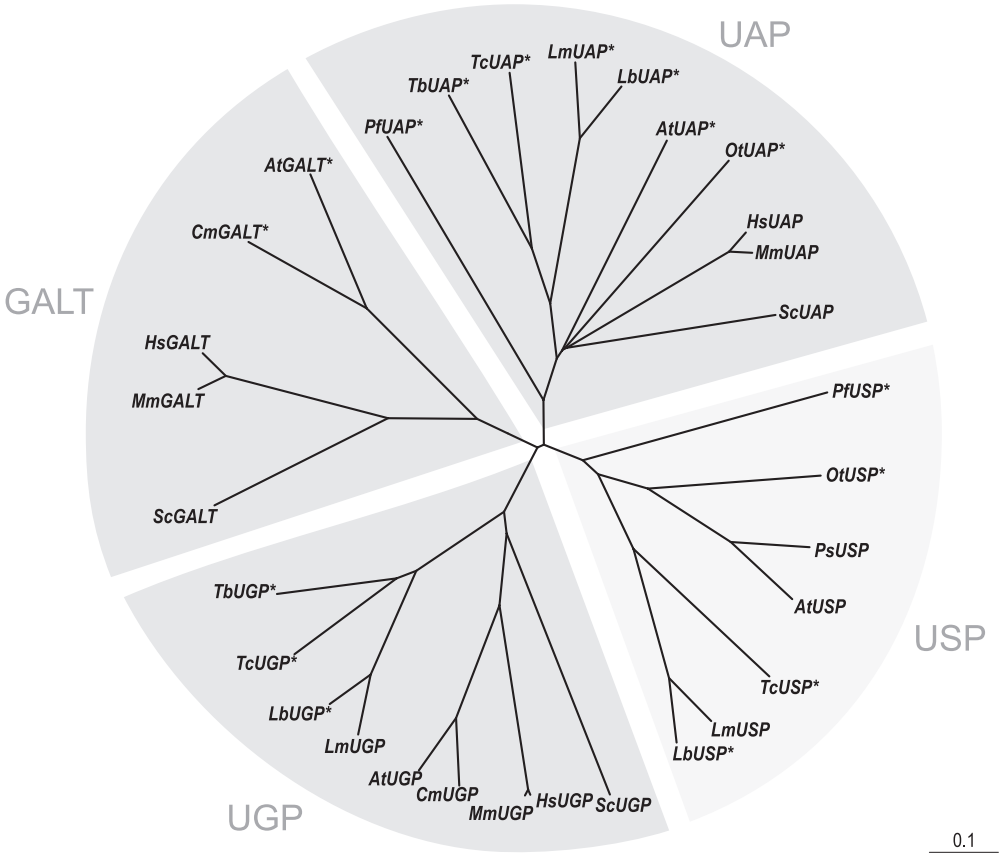

FIGURE 2. **Relation of *L. major* UDP-sugar pyrophosphorylase with UDP-glucose pyrophosphorylases, UDP-GalNAc pyrophosphorylases, and UDP-glucose: α-D-galactose 1-phosphate uridylyltransferases.** *A*, amino acid sequence alignment of *L. major* USP and UGP. Residues involved in UDP-glucose binding of UGP are marked below for contact with the nucleotide (*square*), glucose (*diamond*), or phosphate (*circle*); the pyrophosphorylase consensus sequence is *boxed*. *B*, unrooted phylogenetic tree of selected sequences (EBI-ClustalW2 multiple alignment). The abbreviations used are as follows: *USP*, UDP-sugar pyrophosphorylase (EC 2.7.7.64); *UGP*, UDP-glucose pyrophosphorylase (EC 2.7.7.9); *GALT*, UDP-glucose:α-D-galactose 1-phosphate uridylyltransferase; *UAP*, UDP-GalNAc pyrophosphorylase (EC 2.7.7.23); *At*, *A. thaliana*; *Cm*, *Cucumis melo*; *Hs*, *Homo sapiens*; *Lb*, *Leishmania braziliensis*; *Lm*, *L. major*; *Mm*, *Mus musculus*; *Ot*, *O. tauri*; *Pf*, *Plasmodium falciparum*; *Sc*, *Saccharomyces cerevisiae*; *Tb*, *T. brucei*; *Tc*, *T. cruzi*. Noncharacterized putative proteins are marked with an *asterisk*.

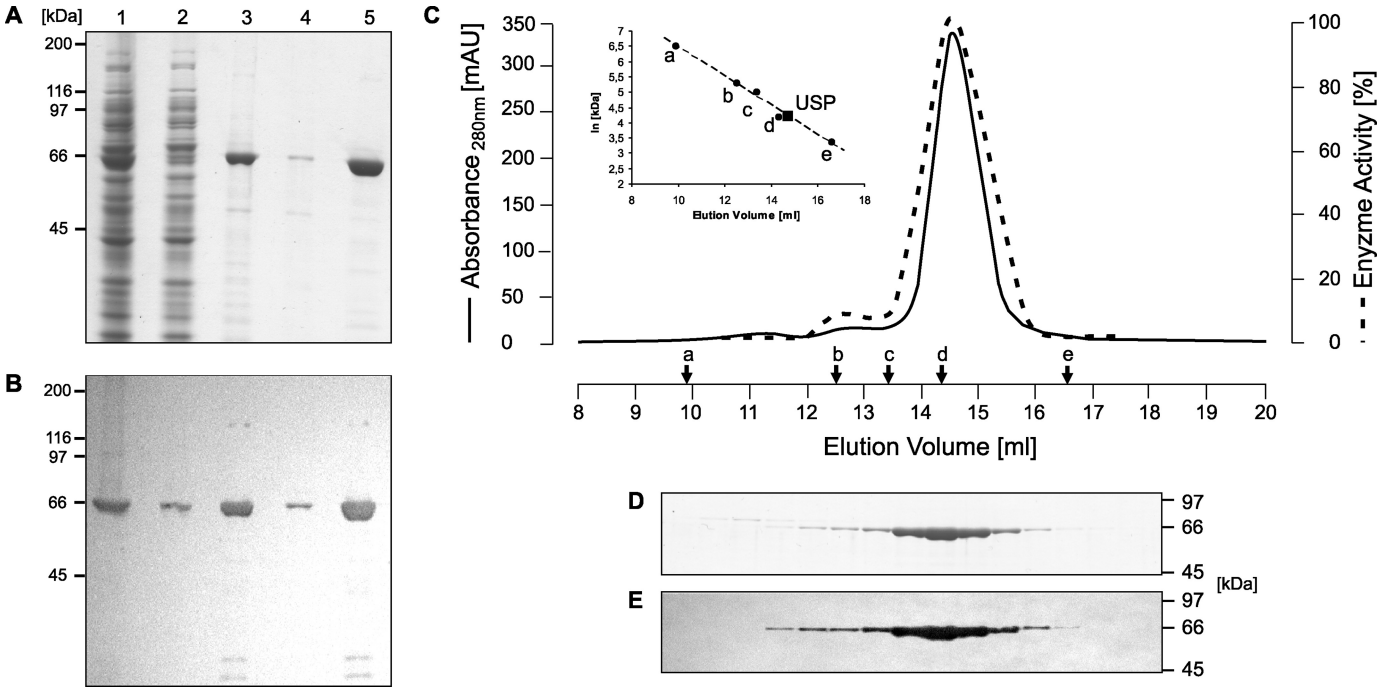

FIGURE 3. **Purification and oligomerization status of recombinant *L. major* UDP-sugar pyrophosphorylase.** Purification of *E. coli*-expressed *L. major* USP-His_6 was followed by SDS-PAGE with Coomassie staining (*A*) and anti-His_6 Western blotting (*B*). *Lane 1,* bacterial lysate; *lane 2,* flow-through of the nickel column; *lane 3,* desalted eluate of the nickel column; *lane 4,* flow-through of anion-exchange column; *lane 5,* desalted eluate of anion-exchange column. Determination of quaternary organization was performed by size-exclusion chromatography (*C*). Protein standards are indicated by *arrows* (*a–e*: 669, 200, 150, 66, and 29 kDa), and the apparent molecular mass of *Lmj*USP-His_6 was determined by standard curve (*inset*). *Lmj*USP-His_6 elutes at a retention volume of 14.65 ml (*solid line*), corresponding to a protein of 69.7 kDa. The activity pattern (*dashed line*) confirms that the monomer is the active form. Elution was traced by SDS-PAGE Coomassie staining (*D*) and anti-His_6 Western blotting (*E*) of fractions.

(Fig. 3). The recombinant *L. major* USP eluted as a single peak at 14.65 ml corresponding to an apparent molecular mass of 69.7 kDa calculated from the log molecular weight *versus* retention volume plot (Fig. 3*C*, *inset*). The theoretical mass (70.4 kDa) to an apparent molecular mass ratio of 1.01 clearly indicates that the recombinant His_6-tagged *Lmj*USP is a monomer. This result was confirmed using untagged *Lmj*USP expressed in *E. coli* and partially purified by anion-exchange and size-exclusion chromatography (data not shown). Moreover, we demonstrated that the monomeric form (identified by PAGE and Western blotting in Fig. 3, *D* and *E*, respectively) is the active form of the enzyme by assaying each fraction for their ability to synthesize UDP-glucose with the assay described below (Fig. 3*C*).

Because of its homology with plant USPs, *Lmj*USP was anticipated to have broad substrate specificity; versatile enzymatic assays that allow testing of the forward or reverse reaction with various substrates were thus established. The synthesis of UDP-Glc, UDP-Gal, or other UDP-sugar from their respective sugar 1-phosphate and UTP (forward reaction) generates pyrophosphate as a by-product that can be monitored using the Enz-Chek pyrophosphate kit (Invitrogen). This system is based on hydrolysis of pyrophosphate and subsequent enzymatic reaction of inorganic phosphate with 2-amino-6-mercapto-7-methylpurine ribonucleoside to produce ribose 1-phosphate and 2-amino-6-mercapto-7-methylpurine absorbing at 360 nm. In pilot experiments, the possibility of ribose 1-phosphate cross-reactions with *Lmj*USP was therefore excluded by competitive testing with the substrate Glc-1-P in a different NADH-based assay system (28) (data not shown). Alternatively, the formation of UTP was followed to analyze the synthesis of sugar 1-phosphate from nucleotide sugar and pyrophosphate (reverse reaction). In this assay, UTP was utilized by *E. coli* CTP-synthase (29) generating free inorganic phosphate that could be detected using the same principle. The substrate specificity of the enzyme was determined by one of the employed *in vitro* assays (Table 1). Gal-1-P and Glc-1-P appeared to be the main substrates of *Lmj*USP, in agreement with the ability of the enzyme to functionally complement *E. coli* DEV6 galU mutants. Like UGP, *Lmj*USP acts reversibly *in vitro* and could efficiently use the substrates UDP-Gal and UDP-Glc to produce Gal-1-P and Glc-1-P, respectively. Importantly, significant activity, albeit at lower level, was also detected when D-xylopyranose 1-phosphate (Xyl-1-P), UDP-β-L-arabinopyranose (UDP-L-Ara), or UDP-α-D-galacturonate (UDP-GalA) was used as substrate, whereas GlcNAc-1-phosphate and UDP-GalNAc were not converted. Similarly, α-D-mannose 1-phosphate (Man-1-P) and α-L-fucose 1-phosphate (Fuc-1-P) were not activated by *Lmj*USP in the presence of GTP. Our results clearly establish that the leishmanial enzyme exclusively utilizes UTP for activation of Gal-1-P in accordance with expectations. Together, these data establish the pyrophosphorylase activity of the candidate protein and demonstrate its broad substrate specificity that includes Gal-1-P and Glc-1-P.

L. major USP Follows Simple Michaelis-Menten Kinetics—The kinetic parameters of the purified enzyme were determined for the main substrates of the forward (Gal-1-P, Glc-1-P, and UTP) and reverse (UDP-Gal, UDP-Glc, and pyrophos-

phate) reaction. Additionally, UDP-L-Ara and UDP-GalA, which represent analogues of UDP-Gal in which the C6 group is either absent or substituted, were analyzed. *L. major* USP followed Michaelis-Menten kinetics with all substrates tested (supplemental Fig. S3). The calculated kinetic parameters V_{max}, K_m, k_{cat}, and derived catalytic efficiency (k_{cat}/K_m) are summarized in Table 2. Interestingly, Gal-1-P seems to be preferred over Glc-1-P (K_m = 860 and 1706 μM, respectively) suggesting a slight influence of the C4 hydroxyl group stereochemistry in substrate binding. Nevertheless, the affinity of *L. major* USP for these two hexose 1-phosphates is rather low and remarkably lower than the affinity of the enzyme for UTP (K_m = 860 and 1706 μM *versus* 98 or 116 μM), the latter being comparable with the affinity of various UGPs for UTP (22, 30, 31). This striking difference is reflected by the low efficiency of the enzyme with hexose 1-phosphates when compared with the co-substrate UTP. In contrast, the affinity and maximum velocity of the enzyme with UDP-Gal and UDP-Glc are comparable (K_m = 148 or 174 μM and V_{max} = 134 or 157 μmol/min/mg, respectively) resulting in an identical efficiency of the enzyme with these two substrates of 51% when compared with the efficiency obtained with UTP. Assuming that the sugar moiety of hexose 1-phosphate and UDP-hexose binds to the same site, the higher affinity of *Lmj*USP for the UDP-sugar suggests that the nucleotide moiety plays a major role in substrate binding. This hypothesis is consistent with the high K_m value for UTP. As expected, the affinity and turnover for UDP-L-Ara and UDP-GalA are low in agreement with the observation that these nucleotide sugars are poorer substrates (Tables 1 and 2) (19, 20, 32). Thus, the absence of the C6 hydroxyl group and particularly its substitution leads to a drastic reduction of the enzyme efficiency.

Because of its high affinity for *Lmj*USP, UTP might bind first to the enzyme followed by Gal-1-P or Glc-1-P thus favoring the forward reaction despite the low affinity of the enzyme for Gal-1-P and Glc-1-P. In line with this assumption, the turnover rates measured for the hexose 1-phosphates were similar to the turnover rate measured for UTP (~200 s^{-1}) and higher than the one of UDP-Gal, UDP-Glc, or pyrophosphate (~170 s^{-1}). Altogether, the kinetic data and their comparison with data obtained with *L. major* UGP (24) suggest an ordered bi-bi substrate mechanism.

L. major USP Follows an Ordered Bi Bi Mechanism—To gain insight into substrate binding to *L. major* USP and substantiate a sequential binding mode of substrates to the enzyme, protein-ligand interactions were investigated by STD NMR. This powerful method (33, 34) is capable of identifying ligand-binding epitopes of a ligand when bound to a target protein. Ligand protons that are in close contact with the enzyme receive a higher degree of saturation via the protein resulting in the observation of stronger STD NMR signals compared with ligand protons that do not interact with the protein surface and are solvent-exposed. ^{1}H NMR spectra were first recorded to assign signals and ensure that the enzyme was active in the forward and reverse reactions under the applied assay condi-

TABLE 1

***L. major* UDP-sugar pyrophosphorylase substrate specificity**

Relative enzymatic activities of purified *Lmj*USP were determined in the presence of different acceptor substrates. All acceptor substrates were used in rate nonlimiting concentrations (3 mM sugar 1-phosphates, 0.8 mM UTP, 2 mM UDP-sugars, and pyrophosphate). The highest activity obtained was set to 100%. Errors are given as standard deviations from triplicate measurements.

	Relative activity
	%
A. Forward reaction (+UTP)	
Sugar 1-phosphate	
Gal-1-P	100 ± 2.6
Glc-1-P	88 ± 6.8
Xyl-1-P	12 ± 1.0
GalA-1-P	1.6 ± 0.1
GlcNAc-1-P	0.6 ± 0.03
Man-1-P	0.007 ± 0.004
B. Reverse reaction (+PP_i)	
UDP-sugar	
UDP-Gal	83 ± 1.2
UDP-Glc	100 ± 4.1
UDP-L-Ara*p*	33 ± 0.3
UDP-GalA	7.1 ± 0.1
UDP-GalNAc	0.013 ± 0.0015
C. Forward reaction (+galactose L-phosphate)	
NTP	
UTP	100 ± 13
CTP	0.2 ± 0.2
ATP	0.7 ± 0.2
GTP	0.3 ± 0.6

TABLE 2

***L. major* UDP-sugar pyrophosphorylase kinetic parameters**

Indicated substrate parameters were determined in presence of rate nonlimiting and constant co-substrate concentrations (0.8 mM UTP, 2 mM Gal-1-P, 3 mM Glc-1-P, 2 mM pyrophosphate, and 2 mM UDP-sugars), in order to generate a pseudo first-order reaction type. The highest efficiency obtained was UTP set to 100% for both directions (A and B). Errors are given as standard deviations from triplicate measurements.

Substrate	K_m	V_{max}	k_{cat}	Efficiency	
				k_{cat}/K_m	%
	μM	μmol/min/mg	s^{-1}	$M^{-1}s^{-1}$	
A. Forward reaction					
Gal-1-P	860 ± 34	190 ± 3	219 ± 3	$2.59 \times 10^5 \pm 1.42 \times 10^4$	12 ± 0.7
Glc-1-P	1706 ± 144	166 ± 6	191 ± 6	$1.14 \times 10^5 \pm 1.34 \times 10^4$	5 ± 0.6
UTP (Gal-1-P)	98 ± 10	175 ± 7	201 ± 8	$2.09 \times 10^6 \pm 2.80 \times 10^5$	100 ± 13.4
UTP (Glc-1-P)	116 ± 18	181 ± 11	209 ± 13	$1.83 \times 10^6 \pm 3.90 \times 10^5$	88 ± 18.7
B. Reverse reaction					
UDP-Gal	148 ± 8	134 ± 2	154 ± 2	$1.07 \times 10^6 \pm 7.18 \times 10^4$	51 ± 3.4
UDP-Glc	174 ± 9	157 ± 3	180 ± 3	$1.06 \times 10^6 \pm 7.18 \times 10^4$	51 ± 3.4
UDP-L-Ara*p*	373 ± 48	63 ± 3	72 ± 4	$1.98 \times 10^5 \pm 3.60 \times 10^4$	9 ± 1.7
UDP-GalA	790 ± 193	11 ± 1	13 ± 1	$1.67 \times 10^4 \pm 5.61 \times 10^3$	1 ± 0.3
PP_i (UDP-Gal)	307 ± 18	152 ± 3	174 ± 4	$5.80 \times 10^5 \pm 4.51 \times 10^4$	28 ± 2.2
PP_i (UDP-Glc)	383 ± 11	161 ± 2	185 ± 2	$4.92 \times 10^5 \pm 1.91 \times 10^4$	24 ± 0.9
PP_i (UDP-L-Ara_p)	1018 ± 112	70 ± 5	81 ± 5	$8.12 \times 10^4 \pm 1.40 \times 10^4$	4 ± 0.7
PP_i (UDP-GalA)	728 ± 113	13 ± 1	15 ± 1	$2.08 \times 10^4 \pm 4.88 \times 10^3$	1 ± 0.2

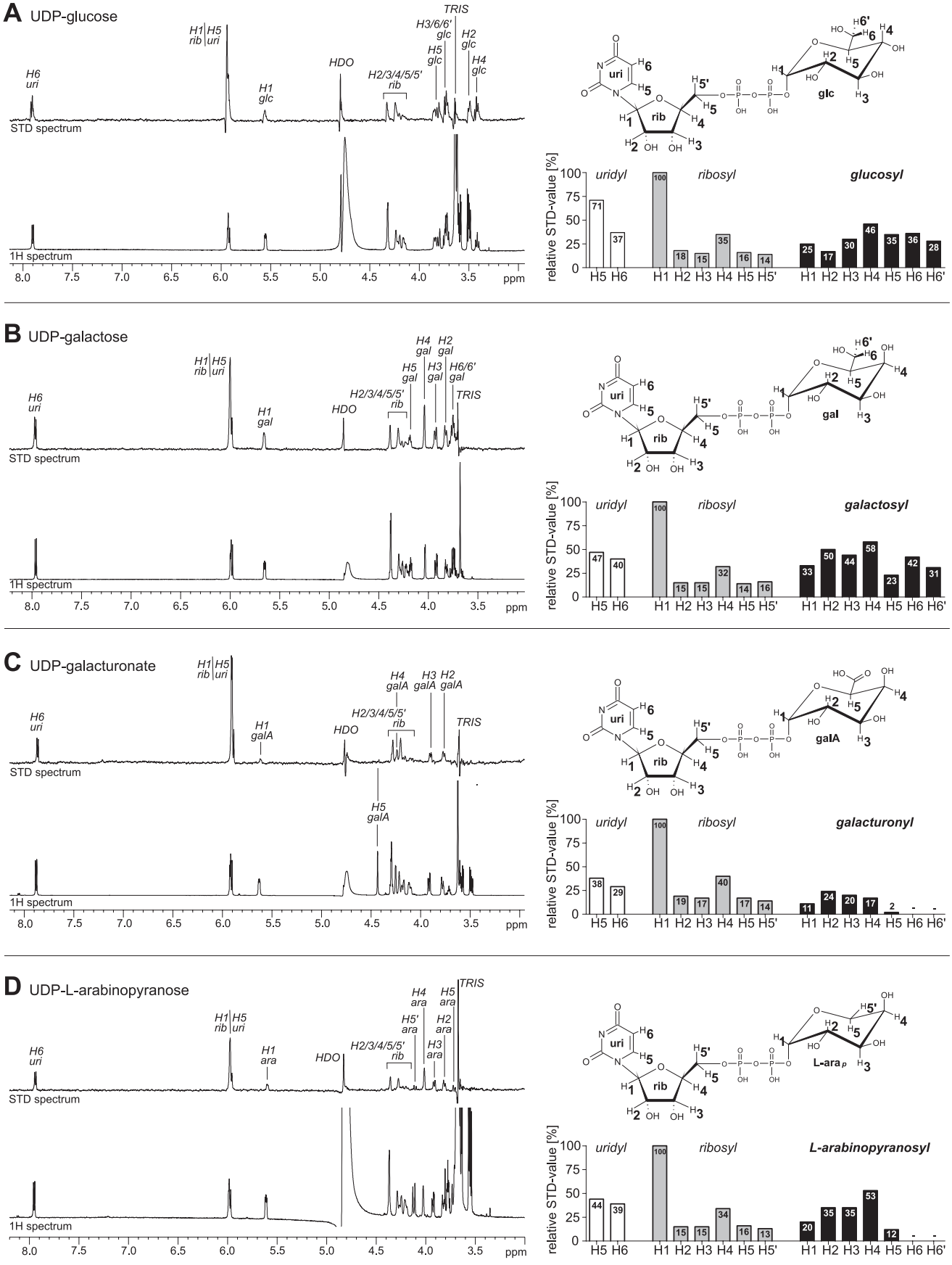

tions. STD NMR experiments revealed strong STD NMR signals for UTP, whereas the related nucleotides ATP, GTP, and CTP result in low, if any, STD NMR signal intensity (supplemental Fig. S4). This result strongly suggests that ATP, GTP, and CTP have low affinity for USP. The clear signals arising from the ribosyl proton $H4_{rib}$, uridyl protons $H5_{uri}$ and $H6_{uri}$, and in particular from the ribosyl proton $H1_{rib}$ of UDP-Gal indicate their close vicinity to the protein surface. Interestingly, UDP and UMP show little affinity for *Lmj*USP emphasizing the importance of the UTP γ-phosphate in binding (supplemental Fig. S5). In contrast, the STD NMR spectra of UDP-Gal, UDP-Glc, UDP-GalA, and UDP-L-Ara display strong STD NMR effects, indicating high affinity (Fig. 4) for *Lmj*USP. The STD NMR spectrum of UTP revealed close proximity of the $H1_{rib}$, $H4_{rib}$, $H5_{uri}$, and $H6_{uri}$ protons when bound to *Lmj*USP, whereas the $H2_{rib}$, $H3_{rib}$, and $H5/H5'_{rib}$ protons seem less important in the binding event. This interaction is strengthened by the sugar moiety notably in the case of UDP-Gal and UDP-Glc. Remarkably, most of the Gal protons are in close vicinity of the protein surface with the $H4_{gal}$, $H2_{gal}$, $H3_{gal}$, and $H6_{gal}$ protons making the most significant contributions to the binding event. In comparison, the glucose moiety of UDP-Glc receives less saturation suggesting a lesser involvement in the binding event to the enzyme. The relative STD NMR effects of the $H1_{glc}$ (25%), $H2_{glc}$ (17%), and $H3_{glc}$ (30%) protons clearly demonstrate a less intimate contact with the protein and therefore a likely poorer affinity of UDP-Glc for USP. Despite their different stereochemistry, the $H4_{gal}$ and $H4_{glc}$ protons show no drastic difference in relative STD NMR effects, in good agreement with the specificity of the enzyme. Finally, the STD NMR spectra of UDP-Ara and UDP-GalA emphasize the importance of the $H6_{gal/glc}$ and $H6'_{gal/glc}$ proton contacts with the protein surface. UDP-Ara seems to bind to the enzyme in a similar manner as UDP-Gal, but loss of H6 and H6′ results in a reduced affinity. In contrast, the steric hindrance and/or negative charge of the carboxylic group of GalA appears to strongly influence binding of the sugar as only weak STD NMR effects in complex with the enzyme are observed.

Interestingly, no binding of Gal-1-P, Glc-1-P, or Xyl-1-P to L*mj*USP was observed by STD NMR spectroscopy. However, addition of UTP to the sugar 1-phosphate/*Lmj*USP mixture resulted in strong and specific STD NMR signals for H4 and H2 protons of Gal-1-P (Fig. 5). This phenomenon, suggestive of an ordered bi-substrate mechanism with UTP binding preceding the hexose 1-phosphate entry, was previously observed with the L*mj*UGP, and a conformational change was proposed (22). The subsequently determined x-ray crystal structure clearly revealed a conformational change upon complexion with UTP (26). It is therefore not unreasonable to assume that USP binds UTP in a similar mode. Interestingly, STD NMR signals could be clearly observed for various UDP-sugars even in the absence of pyrophosphate. In the reverse reaction, the data suggest a sequential binding mode with the nucleotide sugar binding prior to pyrophosphate supported by the observation that the affinity of the enzyme for pyrophosphate seems to be influenced by the nucleotide sugar (Table 2).

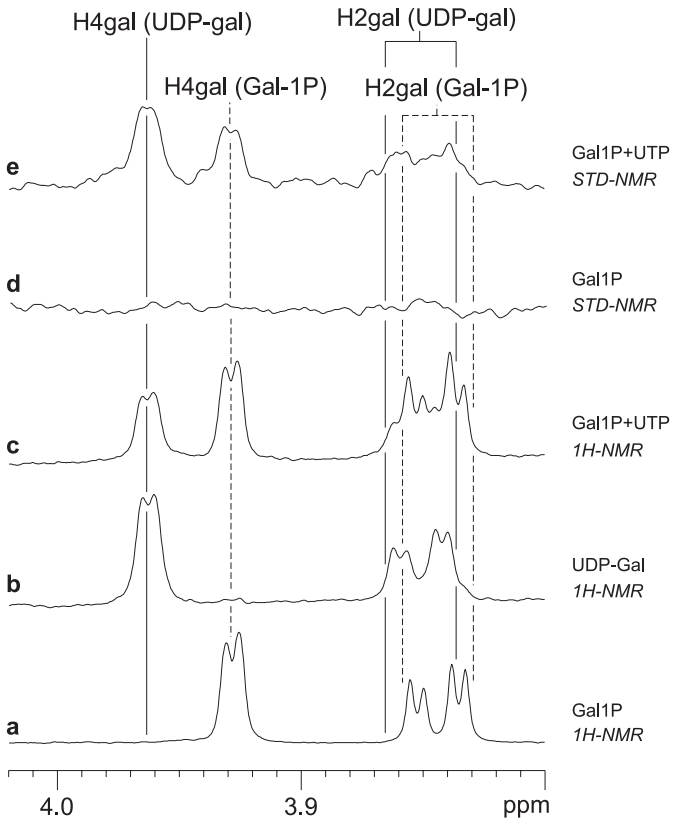

FIGURE 5. **Ordered bi-substrate mechanism of *L. major* UDP-sugar pyrophosphorylase.** STD NMR spectrum for Gal-1-P does not present any signal demonstrating absence of binding to *L. major* USP (*d*). In the presence of UTP, Gal-1-P binds to the enzyme, and UDP-Gal is formed as shown by relative STD NMR signals for these compounds (*e*). ^{1}H NMR spectra of Gal-1-P (*a*); UDP-Gal (*b*) and a mixture of Gal-1-P and UTP showing conversion into UDP-Gal (*c*) were acquired for reference.

DISCUSSION

Although *Leishmania* promastigotes are known to incorporate Gal taken from the environment into surface molecules (15), enzymes involved in the salvage pathway for UDP-Gal synthesis had not yet been reported. The activation of this monosaccharide was lately shown to be independent from UDP-Glc synthesis because an *L. major* UGP deletion mutant still expresses Gal-containing molecules.[5] Herein, we report the identification and characterization of an *L. major* UDP-sugar pyrophosphorylase able to reversibly activate Gal-1-P into UDP-Gal constituting the Isselbacher pathway for UDP-Gal synthesis.

L. major USP presents a clear homology with plant USPs and a modest but significant homology with UGPs and UDP-*N*-

FIGURE 4. **STD NMR spectra of UDP-sugars complexed with *L. major* UDP-sugar pyrophosphorylase.** STD NMR spectra are shown for UDP-glucose (*A*), UDP-galactose (*B*), UDP-galacturonate (*C*), and UDP-L-arabinopyranose (*D*). All spectra were recorded at 298 K, 600 MHz using deuterated Tris buffer (50 mM, pH 7.8) and $MgCl_2$ (10 mM) in D_2O. The on resonance frequency was set to 0.7 ppm and the off resonance to 40 ppm. The residual water signal was removed by applying a WATERGATE sequence. Epitope maps were constructed by calculating relative STD NMR effects according to the formula $A_{STD} = (I_0 \times I_{sat})/I_0 = I_{STD}/I_0$ (see supplemental material) using the $H1_{rib}$ proton to 100% (*bar chart*). Each of the analyzed UDP-sugars shows strong STD NMR signals.

acetylglucosamine pyrophosphorylases over the entire sequence. In particular, the pyrophosphorylase glycine-rich consensus motif (25, 26) essential for catalysis is highly conserved and additional residues involved in uridine and phosphate binding. As highlighted by STD NMR spectroscopic studies, interactions of the uridine moiety of nucleotide sugars or UTP with *Lmj*USP are similar to those observed with *Lmj*UGP and play a significant role in substrate binding. This leading role of the nucleotide moiety is observed in many enzymes involved in glycosylation, for example UDP-galactopyranose mutase (35), sialyltransferases (36), and pyrophosphorylases from *E. coli* (37), and might even hold true for nucleotide sugar transporters (38).

Intriguingly, residues interacting with the glucose moiety in UGPs are not conserved in USPs, which probably accounts for the broader specificity toward monosaccharide 1-phosphates and UDP-sugars of the latter. Like plant USPs, *Lmj*USP is able to convert reversibly and efficiently both Glc-1-P and Gal-1-P with a slight preference for Gal-1-P. Pentose 1-phosphates such as Xyl-1-P and Ara-1-P can also be activated *in vitro* by *Leishmania* or plant USPs, albeit with a reduced efficiency reflecting their lower affinity for the enzyme and underlining the contribution of the hexoses H6 and H6′ protons to binding. In contrast, GalA-1-P is a poor substrate of *Lmj*USP. It is reasonable to assume that the carboxylic acid group of GalA creates either steric hindrance or more likely an unfavored electrostatic potential leading to weak interactions of the uronic acid with the leishmanial enzyme. Different from the plant enzymes, all USPs identified in *Leishmania* species present an 18-amino acid insertion near the uridine-binding site that contains the conserved residues G223H224. Although not yet proven, this insertion might be responsible for the substrate differences observed for plant enzymes. The role of these additional amino acids awaits a crystal structure of *Lmj*USP.

Despite its lower affinity for Ara-1-P, *Arabidopsis thaliana* USP seems to play a central role in the salvage of this pentose *in vivo* (21). In *Leishmania*, however, where D-Ara is present, the monosaccharide is exclusively activated by GDP, and a putative GDP-Ara pyrophosphorylase has been identified in the genome (8). In addition to GDP-α-D-Ara, *L. major* promastigote synthesizes UDP-Glc, UDP-Gal (in the pyranosic and furanosic form), UDP-GlcNAc, GDP-Man, and low amounts of GDP-Fuc, but neither UDP-Xyl nor its precursor UDP-GlcA are produced (8). Considering the specificity of *Lmj*USP for UDP-activated sugars, its inability to act on hexosamine 1-phosphate, and the characterization or presence in the genome of specific pyrophosphorylases for the activation of GDP-activated sugars and UDP-GlcNAc (8, 39), *Leishmania* USPs most likely play a role in the salvage of galactose and glucose exclusively. Moreover, and despite the fact that USP is able to act reversibly, the ordered Bi Bi mechanism of the enzyme and its high affinity for UTP, a naturally abundant metabolite, presumably ensures the synthesis of nucleotide sugar rather than their pyrophosphorolysis. Remarkably, *Lmj*USP seems to have evolved a slight preference for Gal-1-P over Glc-1-P in good agreement with the presence of Gal in many of their surface glycoconjugates.

In contrast to *Leishmania* parasites, the trypanosomatids *T. brucei* and *T. cruzi* are thought to rely exclusively upon epimerization of UDP-Glc for synthesis of UDP-Gal, because the hexose transporters of these parasites are unable to transport Gal (9, 10). Nevertheless, the genome of *T. cruzi* contains homologues of galactokinase and USP, which might be involved in recycling galactose originating from degradation of glycoconjugates in the endo-lysosomal compartment or plays a role in salvage pathways of other sugars. *T. cruzi* is the only one of the three trypanosomatids that synthesizes UDP-Rha, UDP-Xyl, and its precursor UDP-GlcA (8). Like the plant enzyme, *T. cruzi* USP might be involved in the synthesis of these nucleotide sugars. In *Arabidopsis*, USP is particularly important in pollination and possibly converts Gal-1-P, Ara-1-P, and Rha-1-P secreted by the pistil (21). In *T. cruzi,* however, the precise function of the Xyl and Rha metabolism is still unclear.

The trypanosomatid USPs are closely related to plant USPs and hypothetical proteins of the diatoms *Phaedactylum tricornutum* and *Thalassiosira pseudonana* and green algae *Micromonas pusilla*, *Ostreococcus tauri*, *Ostreococcus lucimarinus*, and *Chlamydomonas reinhardtii*, which suggest the common origin of these genes. Moreover, USP homologues are found in ciliate protozoa (*Paramecium tetraurelia* and *Tetrahymena thermophila*) and Apicomplexa (*Toxoplasma gondi*, *Cryptosporidium* sp., and *Plasmodium* sp.) but seem absent from Percolozoa, Loukozoa, and Metamonada. The discovery of a plant-like enzyme common to several pathogens opens new perspectives for the development of a pesticide-like drug as already proposed for the apicomplexan parasites (40). Like in mammals (41) and yeast (42), accumulation of Gal-1-P might reveal toxic for the parasite.

Acknowledgments—We thank Nikolay Nifant'ev (Zelinsky Institute of Organic Chemistry, Russian Academy of Sciences) for gift of xylose 1-phosphate. UDP-galacturonic acid and UDP-L-arabinose were purchased by CarboSource, supported in part by National Science Foundation RCN Grant 0090281.

REFERENCES

1. Naderer, T., Vince, J. E., and McConville, M. J. (2004) *Curr. Mol. Med.* **4,** 649–665
2. Bakker, H., Kleczka, B., Gerardy-Schahn, R., and Routier, F. H. (2005) *Biol. Chem.* **386,** 657–661
3. Beverley, S. M., Owens, K. L., Showalter, M., Griffith, C. L., Doering, T. L., Jones, V. C., and McNeil, M. R. (2005) *Eukaryot. Cell* **4,** 1147–1154
4. Kleczka, B., Lamerz, A. C., van Zandbergen, G., Wenzel, A., Gerardy-Schahn, R., Wiese, M., and Routier, F. H. (2007) *J. Biol. Chem.* **282,** 10498–10505
5. Capul, A. A., Barron, T., Dobson, D. E., Turco, S. J., and Beverley, S. M. (2007) *J. Biol. Chem.* **282,** 14006–14017
6. Capul, A. A., Hickerson, S., Barron, T., Turco, S. J., and Beverley, S. M. (2007) *Infect. Immun.* **75,** 4629–4637
7. Madeira, da Silva, L., Owens, K. L., Murta, S. M., and Beverley, S. M. (2009) *Proc. Natl. Acad. Sci. U.S.A.* **106,** 7583–7588
8. Turnock, D. C., and Ferguson, M. A. J. (2007) *Eukaryot. Cell* **6,** 1450–1463
9. Tetaud, E., Barrett, M. P., Bringaud, F., and Baltz, T. (1997) *Biochem. J.* **325,** 569–580
10. Barrett, M. P., Tetaud, E., Seyfang, A., Bringaud, F., and Baltz, T. (1998) *Mol. Biochem. Parasitol.* **91,** 195–205
11. Roper, J. R., Guther, M. L., Milne, K. G., and Ferguson, M. A. (2002) *Proc. Natl. Acad. Sci. U.S.A.* **99,** 5884–5889
12. Roper, J. R., Güther, M. L., Macrae, J. I., Prescott, A. R., Hallyburton, I., Acosta-Serrano, A., and Ferguson, M. A. (2005) *J. Biol. Chem.* **280,**

19728–19736
13. Urbaniak, M. D., Turnock, D. C., and Ferguson, M. A. (2006) *Eukaryot. Cell* **5,** 1906–1913
14. MacRae, J. I., Obado, S. O., Turnock, D. C., Roper, J. R., Kierans, M., Kelly, J. M., and Ferguson, M. A. (2006) *Mol. Biochem. Parasitol.* **147,** 126–136
15. Turco, S. J., Wilkerson, M. A., and Clawson, D. R. (1984) *J. Biol. Chem.* **259,** 3883–3889
16. Burchmore, R. J., Rodriguez-Contreras, D., McBride, K., Merkel, P., Barrett, M. P., Modi, G., Sacks, D., and Landfear, S. M. (2003) *Proc. Natl. Acad. Sci. U.S.A.* **100,** 3901–3906
17. Feng, X., Rodriguez-Contreras, D., Buffalo, C., Bouwer, H. G., Kruvand, E., Beverley, S. M., and Landfear, S. M. (2009) *Mol. Microbiol.* **71,** 369–381
18. Isselbacher, K. J. (1958) *J. Biol. Chem.* **232,** 429–444
19. Kotake, T., Yamaguchi, D., Ohzono, H., Hojo, S., Kaneko, S., Ishida, H. K., and Tsumuraya, Y. (2004) *J. Biol. Chem.* **279,** 45728–45736
20. Litterer, L. A., Schnurr, J. A., Plaisance, K. L., Storey, K. K., Gronwald, J. W., and Somers, D. A. (2006) *Plant Physiol. Biochem.* **44,** 171–180
21. Kotake, T., Hojo, S., Yamaguchi, D., Aohara, T., Konishi, T., and Tsumuraya, Y. (2007) *Biosci. Biotechnol. Biochem.* **71,** 761–771
22. Lamerz, A. C., Haselhorst, T., Bergfeld, A. K., von Itzstein, M., and Gerardy-Schahn, R. (2006) *J. Biol. Chem.* **281,** 16314–16322
23. Mayer, M., and Meyer, B. (2001) *J. Am. Chem. Soc.* **123,** 6108–6117
24. Lamerz, A. C., Haselhorst, T., Bergfeld, A., Damerow, S., von Itzstein, M., and Gerardy-Schahn, R. (2006) *Glycobiology* **16,** 1143–1144
25. Peneff, C., Ferrari, P., Charrier, V., Taburet, Y., Monnier, C., Zamboni, V., Winter, J., Harnois, M., Fassy, F., and Bourne, Y. (2001) *EMBO J.* **20,** 6191–6202
26. Steiner, T., Lamerz, A. C., Hess, P., Breithaupt, C., Krapp, S., Bourenkov, G., Huber, R., Gerardy-Schahn, R., and Jacob, U. (2007) *J. Biol. Chem.* **282,** 13003–13010
27. Martz, F., Wilczynska, M., and Kleczkowski, L. A. (2002) *Biochem. J.* **367,** 295–300
28. Peng, H. L., and Chang, H. Y. (1993) *FEBS Lett.* **329,** 153–158
29. Bearne, S. L., Hekmat, O., and Macdonnell, J. E. (2001) *Biochem. J.* **356,** 223–232
30. Duggleby, R. G., Chao, Y. C., Huang, J. G., Peng, H. L., and Chang, H. Y. (1996) *Eur. J. Biochem.* **235,** 173–179
31. Meng, M., Wilczynska, M., and Kleczkowski, L. A. (2008) *Biochim. Biophys. Acta* **1784,** 967–972
32. Ohashi, T., Cramer, N., Ishimizu, T., and Hase, S. (2006) *Anal. Biochem.* **352,** 182–187
33. Haselhorst, T., Garcia, J. M., Islam, T., Lai, J. C., Rose, F. J., Nicholls, J. M., Peiris, J. S., and von Itzstein, M. (2008) *Angew. Chem. Int. Ed. Engl.* **47,** 1910–1912
34. Haselhorst, T., Fleming, F. E., Dyason, J. C., Hartnell, R. D., Yu, X., Holloway, G., Santegoets, K., Kiefel, M. J., Blanchard, H., Coulson, B. S., and von Itzstein, M. (2009) *Nat. Chem. Biol.* **5,** 91–93
35. Gruber, T. D., Borrok, M. J., Westler, W. M., Forest, K. T., and Kiessling, L. L. (2009) *J. Mol. Biol.* **391,** 327–340
36. Datta, A. K., and Paulson, J. C. (1995) *J. Biol. Chem.* **270,** 1497–1500
37. Thoden, J. B., and Holden, H. M. (2007) *Protein Sci.* **16,** 432–440
38. Maggioni, A., von Itzstein, M., Tiralongo, J., and Haselhorst, T. (2008) *ChemBioChem* **9,** 2784–2786
39. Garami, A., and Ilg, T. (2001) *EMBO J.* **20,** 3657–3666
40. Goodman, C. D., and McFadden, G. I. (2007) *Curr. Drug Targets* **8,** 15–30
41. Fridovich-Keil, J. L. (2006) *J. Cell. Physiol.* **209,** 701–705
42. de Jongh, W. A., Bro, C., Ostergaard, S., Regenberg, B., Olsson, L., and Nielsen, J. (2008) *Biotechnol. Bioeng.* **101,** 317–326